PAPER

Check for updates

Sodium phosphate solid base catalysts for production of novel biodiesel by transesterification reaction

Zhenglong Zhao,[a] Wenwang Wu,[a] Lihua Jia [ID] *[a] and Xiangfeng Guo [ID] *[b]

The efficient sodium phosphate (Na_3PO_4) solid base catalysts were prepared and applied in the production of novel biodiesel: ethylene glycol monomethyl ether monolaurate (EGMEML) by transesterification. The calcined sodium phosphate catalysts (NaP-T) were characterized using thermogravimetry analysis (TG-DSC), X-ray diffraction (XRD), scanning electron microscopy (SEM) and X-ray photoelectron spectroscopy (XPS) and so on. The effects of calcination temperature of Na_3PO_4 and main reaction parameters such as molar ratio of ethylene glycol monomethyl ether (EGME) to methyl laurate (ML), dosage of catalyst, reaction time and temperature on the yield of EGMEML were examined. The results showed that the maximum yield of EGMEML could reach 90% under 120 °C within 4 h and 5 wt% of Na_3PO_4 calcined at 400°, and the catalysts displayed good stability and recovery. In addition, the kinetics of transesterification reaction was explored and the results showed that the transesterification reaction followed 1st order kinetics when a large excess of EGME was used, the activation energy (E_a) was found to be 40.2 kJ mol^{-1}.
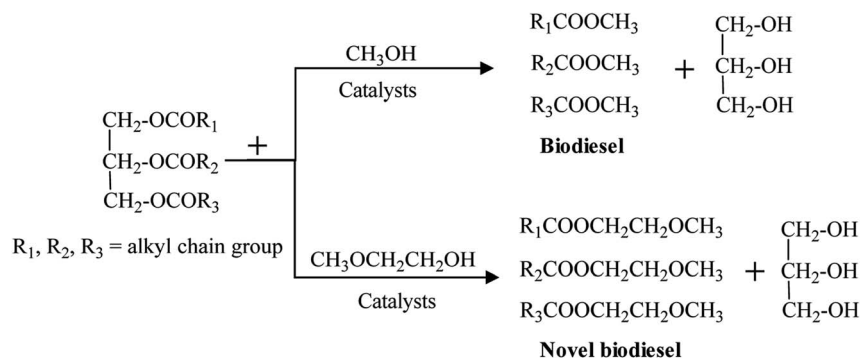
Introduction

Energy shortages and environmental pollution have become the main restricting factors for development of human society. Looking forward, replacing the traditional fossil fuels with renewable and sustainable energy sources has risen to the level of urgency for human development.[1–3] Biodiesel, a mixture of fatty acid methyl esters (FAMEs), obtained from transesterification of vegetable oil or animal fats with alcohol (methanol and ethanol) has similar physical and chemical properties to traditional diesel oil, such as flash point, density, cetane rating and so on.[4] Hence biodiesel, as a sustainable and renewable energy source, has been considered to be the ideal fuel to replace fossil fuels. As well, some researchers have demonstrated that the engine performance of biodiesel in diesel engines exhibited lower harmful gas emissions including particulate matter (PM), volatile organic chemicals (VOCs), carbon monoxide (CO), hydrocarbon (HC) compared with the traditional petroleum diesel oil.[5–7] Wang *et al.*[8] conducted an engine performance test for the cottonseed oil biodiesel and found that the emission of CO, CO_2 and NO_x from cottonseed oil biodiesels was lower than that from diesel fuel, CO decreased by 13.8%, CO_2 by 11.1% and NO_x by 10%.

To improve the combustion performance of biodiesel and reduce the exhaust emissions further, some researchers designed and synthesized a type of novel biodiesel containing an ether group in the molecule through transesterification reaction using vegetable oils and ethylene glycol ether derivatives (methoxyethanol, dimethoxyethane).[9] In general, common biodiesel has only one ester group (shown in Scheme 1), with two oxygen atoms in its molecule, whereas the novel biodiesel has three oxygen due to the introduction of the ether group, and its oxygen content would reach approximately 14–18%, which proved to be more complete combustion, and meanwhile could further reduce the production and emission of polluted gas.[10] Liu *et al.* synthesized the novel biodiesel ethylene glycol *n*-propyl ether palm oil monoester (EGPEPOM) through transesterification of refined palm oil and ethylene glycol *n*-propyl. And the experimental results showed that the smoke emissions of CO, HC, and NO_x were reduced by 37.5, 66.6, 27.1, and 23.7%, respectively.[11] Ethylene glycol monomethyl ether cottonseed oil monoester (EGMECOM) was designed and synthesized by Zhu[12] *et al.*, and the research results indicated that EGMECOM possessed a higher cetane number and oxygen content. And compared with the diesel fuel, the smoke emissions of NO_x, CO, and HC gas decreased by 50.0%, 20%, and 55.6%, respectively.

Homogeneous base catalysts are most widely applied in the transesterification reaction to prepare biodiesel in industrial fields, for example KOH, NaOH.[13,14] And the production process could achieve high yields for biodiesel (98%) within a short reaction time at low temperature.[15] Although, some disadvantages also limited its application in transesterification further,

[a] College of Chemistry and Chemical Engineering, Qiqihar University, Qiqihar 161006, P. R. China. E-mail: jlh29@163.com; xfguo@163.com

[b] College of Chemistry, Guangdong University of Petrochemical Technology, Maoming, Guangdong 525000, P. R. China

Scheme 1 Chemical equation of biodiesel and novel biodiesel production through transesterification reaction.

Table 1 Colour and H_- value of some Hammett indicator

| Indicator	Basic colour	Acid colour	H_-
Bromthymol blue	Yellow	Blue	7.2
Phenolphthalein	Pink	Colourless	9.8
2,4-Dinitroaniline	Red	Yellow	15.0
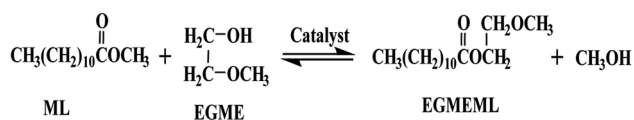
Scheme 2 Transesterification equation of ML with EGME.

including difficulty in separating the products and catalysts, production of caustic wastewater, and serious saponification during the reaction.

To resolve the above problem, heterogeneous solid base catalysts were exploited owing to their high catalytic activity like homogeneous base catalysts, easy recovery and reuse after catalytic reactions and their more environmental-friendly manner.[16–18] Currently the heterogeneous base catalysis reactions used in industrial production are

conducted by the French Institute of Petroleum, in this process the Zn and Al oxide mixture as the solid base catalysts, operated temperature at 200–250 °C, and the maximum yield of production could reach 98.3%.[19] Of course, heterogeneous catalysts also face the following problems: (i) Mass transfer resistance between catalysts and reactants, further leading to the low reaction rate and the need for longer reaction time to obtain the high yield; (ii) active species leaching and catalysts partially dissolving into the reaction mixture during the reaction. Hence much effort has been devoted to design and synthesize solid base catalysts with high activity and good stability, such as metal oxides, hydrotalcite, supported solid bases, phosphates, and so on.[20–24]

Among the solid base catalysts, sodium phosphate (Na_3PO_4) showed great potential for application in the transesterification reaction, owing to high catalytic performance, stable chemical structure, good reusability, and being cheaper to obtain and more environmentally friendly. And Na_3PO_4 has been used in the transesterification reaction to prepare the biodiesel FAMEs.[25–27] Thinnakorn et al.[28] utilized Na_3PO_4 solid base catalysts to produce biodiesel FAMEs via transesterification reaction of palm olein and methanol. In the optimal experimental conditions, 98.5% FAMEs yield was obtained, meanwhile the Na_3PO_4 does not appear to dissolve during the transesterification process.
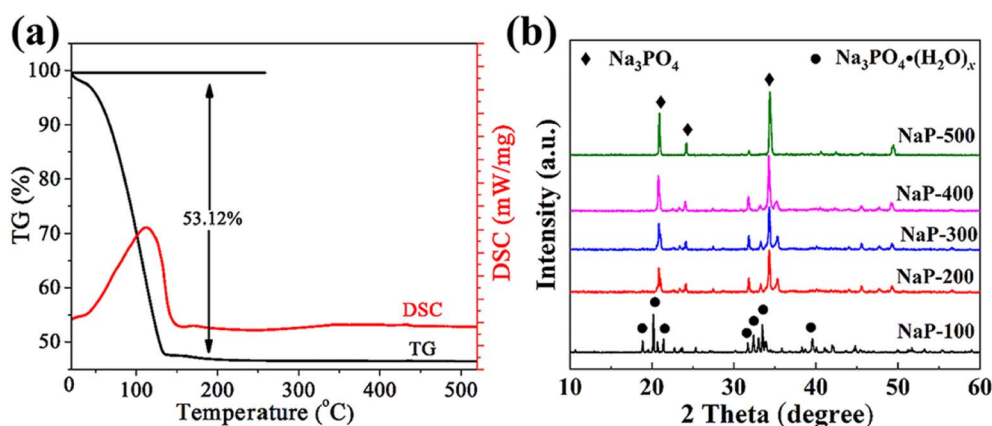
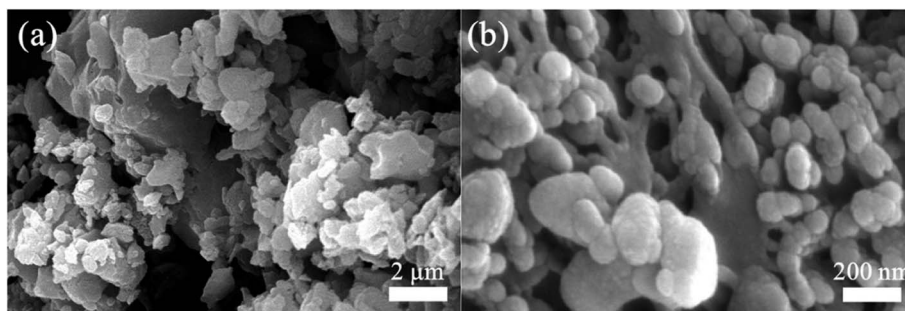**Fig. 1** (a) TG–DSC images; (b) XRD spectra of Na-T catalysts.

Fig. 2 SEM images of NaP-400 under different magnification.

Hence in present work, Na_3PO_4 solid base catalysts were prepared by calcinating the commercial hydrated sodium phosphate and applied in novel biodiesel production, namely ethylene glycol monomethyl ether monolaurate (EGMEML), *via* transesterification reaction between ethylene glycol monomethyl ether (EGME) and methyl laurate (ML). The effects of calcination temperature and main reaction parameters on the yield of EGMEML were examined. The structure of as-prepared samples was characterized by thermogravimetric analysis (TG-DSC), X-ray powder diffraction (XRD), scanning electron microscopy (SEM), X-ray photoelectron spectroscopy (XPS) and the Hammett indicator method. Furthermore, the stability and reusability of the catalyst was studied. The results display that Na_3PO_4 is an effective solid base catalyst in the novel biodiesel production, and could achieve 90% yield for the EGMEML under relatively low

temperature (120 °C), in addition the Na_3PO_4 catalysts exhibit excellent stability and reusability.

Experimental

Materials

Sodium phosphate hydrate, methyl laurate and ethylene glycol monomethyl ether were of analytical grade, and purchased from Aladdin, China.

Catalyst preparation

Sodium phosphate hydrate ($Na_3PO_4 \cdot 12H_2O$) were calcinated at different temperatures for 4 h, respectively, and ground into the fine powder carefully. After that, the powder was sifted through the 80–100 mesh, so the particle size of catalysts was between 150
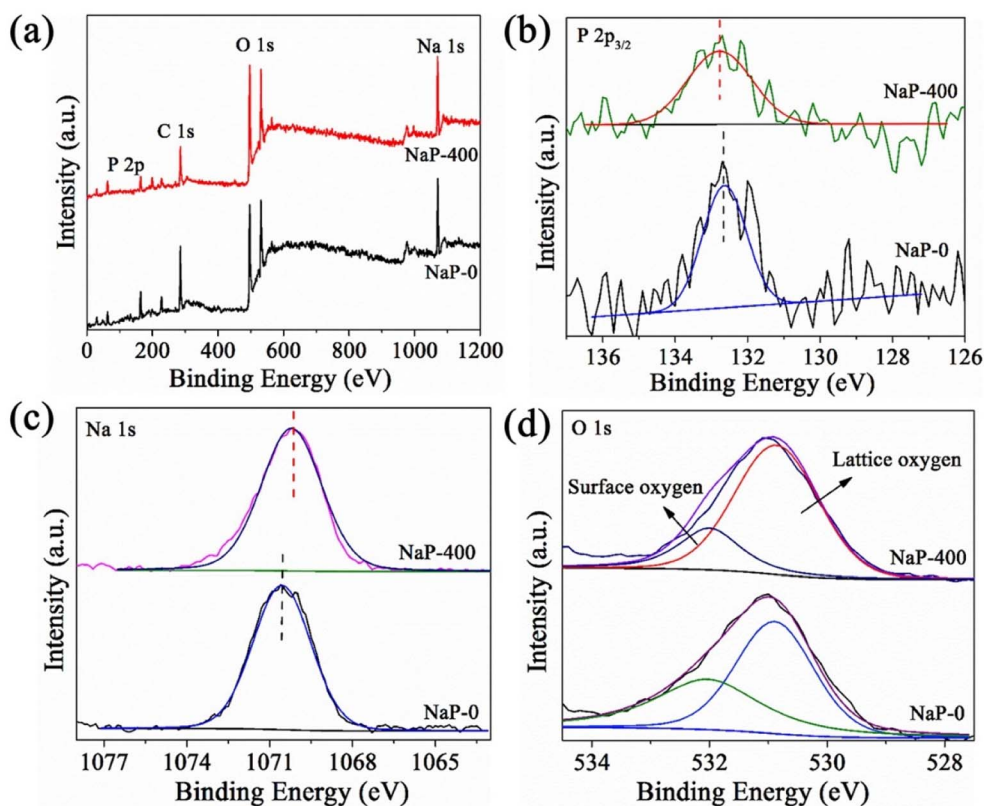

Fig. 3 XPS profiles of (a) full spectrum, (b) P 2p, (c) Na 1s, and (d) O 1s for NaP-400 and NaP-0.

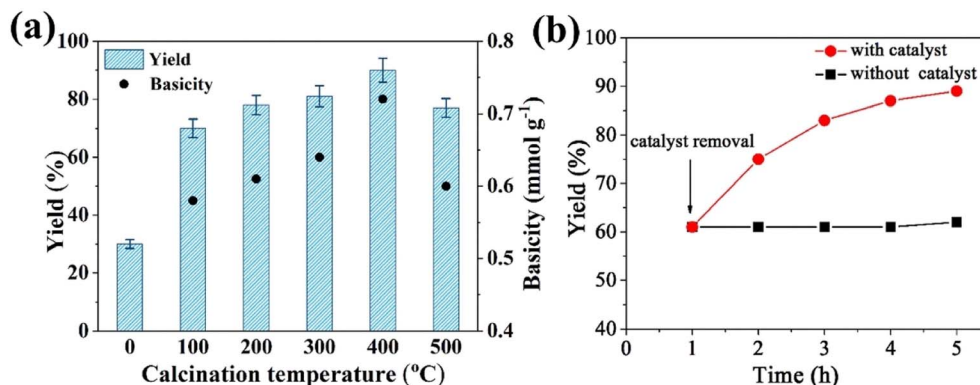© 2023 The Author(s). Published by the Royal Society of Chemistry

Fig. 4 (a) Yield of EGMEML and basicity of catalysts under different calcination temperature; (b) leaching test for NaP-400 catalyst.

and 180 μm. The obtained catalysts were denoted as NaP-*T*, where *T* represents the calcined temperature, the uncalcined sodium phosphate is named NaP-0.

Catalyst characterization

TG–DSC plots were obtained using NETZSCH STA F3, and alumina was used as reference. TG and DSC curves were obtained from 25 to 600 °C under nitrogen atmosphere with the heating rate of 10 °C min⁻¹. XRD experiments were performed on a Bruker D8 Advance diffractometer, using Cu K$_\alpha$ radiation ($\gamma = 1.5418$ Å) at 40 kV and 50 mA. SEM images were obtained with a Rigaku S-4300 spectrometer. The voltage was 20 kV and the vacuum degree

of sample room was better than 10^{-4} Pa. XPS curves were measured using a Kratos-AXIS ULTRA DLD. Aluminium (Mono) as the X-ray source. FT-IR spectra were recorded on an AVATAR370 spectrometer in the range of 4000–400 cm⁻¹. The KBr pellet was applied for preparing samples.

Basic strength of the sample (H_-) was determined by Hammett titration. About 10.0 mg of solid base catalysts were dispersed in 5.00 mL cyclohexane, then two drops of Hammett indicator-benzene solution (0.1%, w/w) were added and equilibrated until no color changed any more. Colors and H_- values of Hammett indicators and the corresponding H_- values are listed in Table 1. Basicity (mmol g⁻¹) of the samples were determined by Hammett
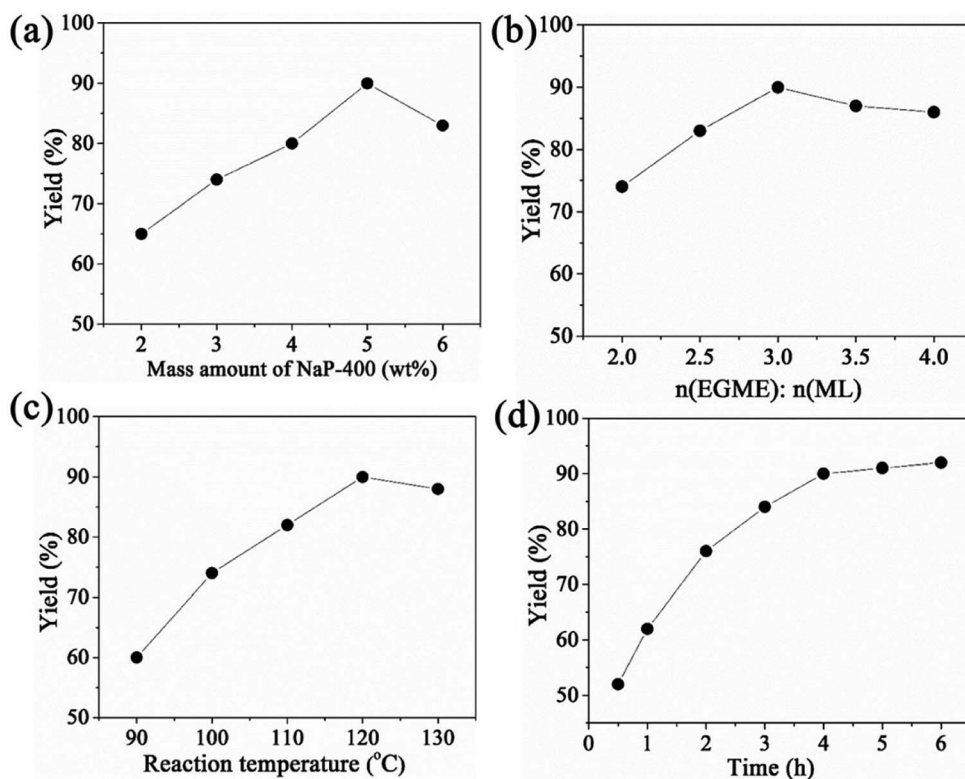

Fig. 5 Influence of reaction conditions on the yield of EGMEML: (a) mass amount of catalyst, (b) molar ratio of EGME/ML, (c) reaction temperature, (d) reaction time used NaP-400 as catalyst.

Table 2 Koros–Nowak test for heat and mass transfer limitations[a]

Catalyst amount (wt%)	Total basic sites (mmol)	TOF (mol min^{-1} mol^{-1})
2	0.0616	1.17
3	0.0924	1.16
4	0.1233	1.17
5	0.1540	1.15

[a] Reaction conditions: molar ratio of EGME to ML is 3.0, reaction temperature at 120 °C, and yield at 40%.

method involving titrated by benzene carboxylic acid indicator (0.02 mol L^{-1} ethanol solution) and until the original colour recovery again.

Catalytic activity measurements

The transesterification reaction equation is shown in Scheme 2. Desired dosages of ML, EGME, and catalyst (on the basis of the weight of ML and EGME) were put into the glass bottle with three necks, which equipped with the thermometer and water-cooled condenser and protected by the nitrogen. Commonly, 4.28 g ML (0.02 mol), 4.56 g EGME (0.06 mol) and 0.46 g NaP-T (wt 5%). Then, the reaction system was stirred and raised to the desired temperature for the certain time. After the reaction finished, the reaction mixture was dipped in the ice bath to cool down the temperature, and centrifuged to separate the catalyst and product. The separated crude products were evaporated in vacuum to remove excess EGME and methanol.

Under unspecified circumstances, the transesterification reaction conditions as following: amount of catalyst 5.0%, reaction time 4 h, molar ratio of EGME/ML of 3.0, reaction temperature of 120 °C.

The residue was analyzed by gas chromatograph (GC9800) furnished with FID detector and OV-17 (30 m × 0.25 mm × 0.25 μm) capillary column. Flow rate of N$_2$ is 50 mL min^{-1}, the temperature of injector, oven, and detector were 280 °C, 250 °C, and 250 °C, respectively. Per injection volume was 0.05 μL. The theoretical mass (m_2) of target product (EGMEML) was calculated by the eqn (1).

$$m_2 = \frac{m_0 - \omega_1 m_1}{M_{ML}} \times M_{EGMEML} \tag{1}$$

The yield (Y) was determined by the following eqn (2).

$$Y = \frac{\omega_2 m_1}{m_2} \times 100\% \tag{2}$$

where m_1 is the residual liquid mass after evaporated (g), m_0 is the initial mass of ML before reaction, M_{ML} and M_{EGMEML} are the molar mass of ML and EGMEML (g mol^{-1}); ω_1 and ω_2 are the mass concentration of the ML and EGMEML in the residual liquid, which determined by the data of gas chromatograph.

The turnover frequency (TOF) was calculated by the following eqn (3).

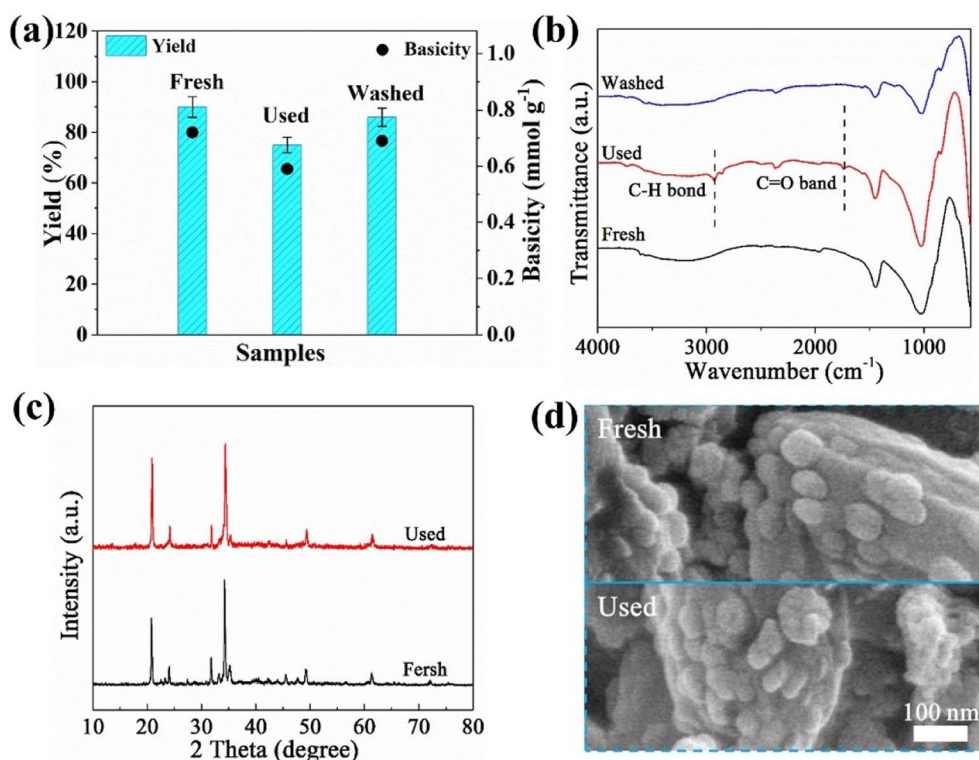$$TOF = \frac{mol_{actual}}{t \times f_m \times m_{cat}} \tag{3}$$

Fig. 6 (a) Yield and basicity, (b) FT-IR spectra of fresh catalyst, used, and washed catalyst, respectively; (c) XRD patterns, (d) SEM images of fresh and used catalyst.
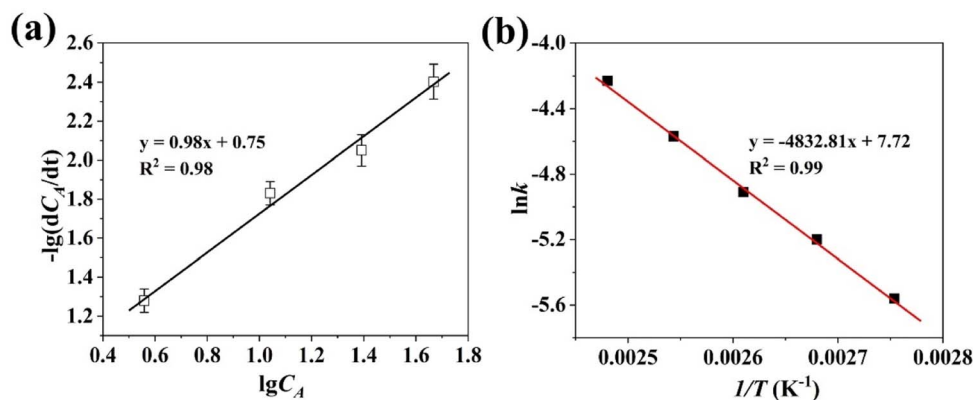
Fig. 7 Transesterification reaction kinetics analysis catalysed by NaP-400 (a) plot of $-\lg(dC_A/dt)$ vs. $\lg C_A$, (b) plot of $\ln k$ vs. $1/T$.

where m_{cat} is the mass dosage of the catalyst (g), mol_{actual} is the mole dosage of target product, t is the desired reaction time (min), and f_m is the dosage of basic sites of the NaP-400 (mmol g^{-1}), which obtained from Hammett method.

The kinetic tests were conducted when the EGME mass was in a large excess (the molar ratio of ML to EGME is 1 : 5). Analytical error was checked by repeating the process 3 times and was found to be less than 2% on average (at 95% confidence error). The experimental error was determined by repeating the experiment 3 times. The errors are shown in the experimental result in the present work.

Results and discussion

Characterization of catalyst

Thermal analysis was performed to investigate the mass and heat variation of sodium phosphate hydrate during the calcination process. As shown in Fig. 1(a), the TG profile has only one weight loss step ranging from 30 °C to 200 °C, which attributed to the loss of crystal water (53.2%), and endothermic peaks accompanied in the relevant DSC profile, it is found that every hydrated sodium phosphate has 11.21 water molecules through calculated the percent of weight loss, which consistent with theoretical quantity. The TG curve has not changed any more in the range from 200 to 500 °C, indicated that no decomposition occurred for sodium phosphate during the calcination from 200 to 500 °C.

Fig. 1(b) is the XRD profiles of sodium phosphate calcinated at different temperature. Firstly, the diffraction peaks appeared at the 2 theta of 18.9°, 20.2°, 21.4°, 31.7°, 32.4°, 33.4°, 39.6° for the NaP-100, which assigned to the characteristic diffraction peak of sodium phosphate hydroxy (JCPDS file number 76-2182). For the NaP-200, most diffraction peaks of the sodium phosphate hydroxy disappeared, the characteristic diffraction peaks of sodium phosphate (JCPDS file number 30-1233) appeared at the 2 theta of 20.9°, 24.1°, 31.3°, 34.2° obviously. And the diffraction peaks became stronger with the calcination temperature increasing from 200 °C to 500 °C. The results show that the thermal treatment could make the crystal phase transformation from the $Na_3PO_4 \cdot (H_2O)_x$ to Na_3PO_4.

The morphological feature of NaP-400 was visualized by the SEM and shown in Fig. 2. The nanosheet and aggregated bulk structure were found for NaP-400 in Fig. 2(a), further the aggregated bulk structure consisted of nanoparticles with the size about 20–50 nm from Fig. 2(b).

To understand the effect of calcination on the element chemical environment of sodium phosphate, the XPS experiments were conducted before and after calcination and the results were shown in Fig. 3. Compare with uncalcined sodium phosphate (NaP-0), the binding energy (BE) of P 2s for NaP-400 increased slightly and the BE of Na 1s exhibits negative shift (Fig. 3(b) and (c)). The O 1s fine spectra (Fig. 3(d)) for NaP-0 and NaP-400 could be deconvoluted into two peaks at 532.0 and 530.8 eV, which are assigned to surface oxygen including the adsorbed and hydroxyl oxygen, and lattice oxygen, respectively. It is noticeable that the content of surface oxygen drops from 43.5% to 23.0% after calcination, suggesting the calcination

Table 3 Transesterification catalytic performance parameters under different solid base catalysts[a]

Catalysts	Products	Reaction conditions	Yield (%)	TOF (min^{-1})	E_a (kJ mol^{-1})	Reference
Na$_2$SiO$_3$	EGMEML	2 : 1, 120 °C, 6 h	90	0.82	50.05	10
CaO	EGMEML	2 : 1, 120 °C, 6 h	73.4			10
KOH	EGMEML	2 : 1, 120 °C, 6 h	48.6			10
Mg–Al hydrotalcite	Biodiesel	48 : 1, 60 °C, 6 h	92			35
Na$_3$PO$_4$	Biodiesel	18 : 1, 210 °C, 0.5 h	98.5		32.59	28
Na$_3$PO$_4$	EGMEML	3 : 1, 120 °C, 4 h	90	1.15	40.2	This work

[a] Reaction conditions: molar ratio of methanol to oil or EGME to ML, reaction temperature (°C) and reaction time (h).

Table 4 Properties of the obtained EGMEML and diesel and biodiesel

Specification	Density/g cm⁻³ (15 °C)	Kinematic viscosity/mm² s⁻¹ (40 °C)	Flash point/°C	Heating value/kJ kg⁻¹	Reference
Diesel	0.838	4.50	64	42.9	33
Biodiesel	0.860–0.900	3.5–5.0	>120	35	34
EGMEPM	0.898	5.98	190	38.2	7
EGMEML	0.905	3.60	133	38.4	This work

process would reduce the amount of surface oxygen including hydroxyl groups and adsorbed oxygen.

Catalytic performance of catalysts

As the solid base catalyst, Na_3PO_4 samples were applied in the transesterification reaction of EGME with ML to prepare EGMEML. As seen in Fig. 4(a), the yield of EGMEML was only 30% using uncalcined Na_3PO_4 (NaP-0) as catalyst. The yield of EGMEML initially increased with increasing the calcination temperature of Na_3PO_4, when the calcination temperature increased to 400 °C, NaP-400 exhibited the maximum yield of 90% for the EGMEML. However, as the calcination temperature increased to 500 °C further, the yield decreased to 77%.

Basic strength and basicity of solid base catalyst are important parameters for the transesterification reaction, so the basic strength and basicity of NaP-T catalysts were measured by the Hammett titration method. The basic strength of NaP-T catalysts is similar, the H_- values are in the range of 9.8–15.0. Whereas the variation of basicity is noteworthy, the basicity enhances with increasing the calcination temperature, NaP-400 achieved the maximum basicity (0.72 mmol g⁻¹), and the calcination temperature increases to 500 °C, the basicity reduces significantly. It is notice that the variation tendency of basicity is consistent with the yield of EGMEML, and the correlation analysis is also shown in Fig. 4(a). Based on above results, it is induced that the calcination process could be change the basicity of sodium phosphate effectively, and the basicity further affects the reactivity and yield of transesterification.

To investigate the heterogeneous nature of the catalyst, the leaching test was conducted used NaP-400 as catalyst. After reacting for 1 h, the catalyst was removed by centrifugation and the reactants were heated up to reaction temperature (120 °C) again for an additional 4 h. As presented in Fig. 4(b), EGMEML yield have no significant change after removing the catalyst. In contrast, the yield of EGMEML increased obviously with the reaction time when adding the catalyst. It illustrated that the transesterification catalyzed by NaP-400 was the typical heterogeneous process.[29]

Influence of the reaction parameters toward catalytic performance

To optimize the reaction conditions of transesterification, different reaction parameters were conducted and the experiment data are shown in Fig. 5. Firstly, the effect of mass amount of catalyst on yield was investigated ranged from 2 wt% to 6 wt%. With the increase of catalyst dosage, the yield of EGMEML increased, and when the mass amount of catalyst is 5 wt%, the yield reached to 90%. Whereas the excessive catalyst dosage was disadvantage for the production of EGMEML, decrease of the EGMEML yield was observed when the catalyst dosage is beyond 5%. It may be due to the high viscosity of the slurry causing the mixing problem involving the reactants, products and catalysts.[30] Therefore the 5 wt% catalyst dosage was selected for the transesterification reaction.

It is a reversible reaction for the transesterification of EGME with ML, so the molar ratio of EGME and ML would influence the reaction balance, and the yield of EGMEML is shown in Fig. 5(b) under different molar ratio of EGME and ML. When the molar ratio of EGME to ML is 3 : 1, the highest yield of 90% was obtained. Increasing the molar ratio of EGME to ML continuously, the yield was decreased slightly. Thus, the molar ratio of EGME to ML located at 3 : 1 for optimum reaction conditions. The effects of reaction temperature and time on the EGMEML yield are seen in Fig. 5(c) and (d). The optimal reaction temperature is 120 °C, and the EGMEML yield achieved to 91%. And when the reaction time was 4 h, the reaction reached the equilibrium state, the yield is 90%, continue to increase the reaction time, the yield increased slowly.

Koros–Nowak test

In order to identify the effect of diffusion limitation on the catalytic activity, Koros–Nowak criterion test was performed.[31] In the present work, different catalyst dosages of NaP-400 were employed in the production of EGMEML, the yield of EGMEML were quantified with time gap of 15 min during the reaction process. As shown in Table 2, the values of TOF almost unchanged with the increase of catalyst dosage significantly, it could be confirmed that the reaction of ML with EGME is immune to the effect of diffusion limitations.

Reusability and recovery of catalysts

Reusability and recovery are the very important factors for the industrial viability of solid base catalysts using in the synthetization of novel biodiesel. Therefore, the recovery property of NaP-400 was evaluated as the typical catalyst.

The used catalyst represents the fresh NaP-400 already had used 12 h in the transesterification reaction continuously after centrifugation and dry. The washed catalyst is the used catalyst after the process of acetone washing. Then the EGMEML yield of fresh and used catalysts were seen in Fig. 6(a), the EGMEML yield of used NaP-400 dropped to 75%, meanwhile, it was found

that the total basicity of used NaP-400 decreased to 0.59 mmol g^{-1}, compare with that of the fresh catalyst of 0.72 mmol g^{-1}, it is maybe resulted from that the basic site on the surface of catalyst were covered by the organics production of transesterification.

Further the FT-IR spectroscopy of the fresh and used catalysts were conducted to analyze the surface structural changes, as shown in Fig. 6(b). Compared the fresh catalyst, new peaks appeared at 1631–1731 cm^{-1}, 2840–2920 cm^{-1} for the used NaP-400, which attributed to C=O and C–H stretching vibrations.[32] It also confirmed that the surface of catalyst was covered by the organics from production. When utilized acetone washing to regenerate the catalyst, the EGMEML yield returned back 86% and the basicity also recovered to 0.69 mmol g^{-1} in Fig. 6(a), meanwhile, the peaks of C=O and C–H stretching vibrations almost disappeared in the FT-IR spectroscopy (Fig. 6(b)), those illustrated acetone-washing could remove the organics of catalysts. The crystalline structure and morphology feature of the fresh and used catalyst were investigated and shown in Fig. 6(c) and (d). It is found that the crystalline degree and appearance have few changes for catalysts before and after use, which implied the NaP-T solid base catalyst possessed the good structural stability in the transesterification of novel biodiesel.

Kinetics study of transesterification reaction

The kinetics study of transesterification reaction for NaP-400 was researched and reaction equation was described as following:

$$ML(A) + EGME(B) \rightarrow EGMEML + MeOH$$
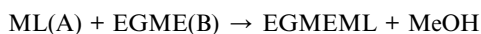
and reaction rate equation could be written as the eqn (4).

$$-\frac{dC}{dt} = k[C_A]^a[C_B]^b \tag{4}$$

where dC/dt is the reaction rate, C_A is ML concentration and C_B is EGME concentration at different reaction time, k is the rate constant, a and b represent the reaction order. As the EGME mass is excess compared with the ML in this work, the $C_{B0} \gg C_{A0}$ was adopt in this kinetics study, namely the molar ratio of ML to EGME is 1 : 5. And C_B could be regard as the constant, C_A could be determined by the GC analysis, further the both side of eqn (4) can be written as the logarithmic model.

$$-\lg \frac{dC_A}{dt} = \lg k + a \lg C_A \tag{5}$$

where the dC_A/dt is the reaction rate, which could obtain from the slope of C_A vs. reaction time (t) curves. The plot of $-\lg(dC_A/dt)$ vs. $\lg C_A$ was shown in Fig. 7(a), and exhibited the good linear correlation, the values of a and k could be obtained from the slope and intercept of curves, respectively. It is found that the numerical values of a was 0.98, which indicated that the grading numbers of reactants A was 1 and the transesterification reaction follows one-order kinetics when the EGME is excess, the eqn (4) could write as following:

$$-\frac{dC}{dt} = kC_A \tag{6}$$

To estimate the activation energy (E_a), the transesterification reaction was conducted under different temperature, and the Arrhenius equation was as following:[31]

$$\ln k = \ln A - E_a/RT \tag{7}$$

which E_a is the activation energy, A is the preexponential factor, R and T represent the gas constant and reaction temperature, respectively.

The graph of $\ln k$ vs. $1/T$ was shown in Fig. 7(b), the value of E_a was 40.2 kJ mol^{-1} through calculation, which was greater than 25 kJ mol^{-1}, it infers that the transesterification reaction is governed by chemical step rather than limited by diffusion under the present study.[32]

Transesterification parameters of different solid base catalysts were listed in Table 3, it is seen that Na_3PO_4 catalysts possessed the lower value of E_a compared with Na_2SiO_3,[10] it illustrated that Na_3PO_4 is easier to conduct the transesterification reaction. And the higher yield of EGMEML was obtained under milder reaction conditions used the Na_3PO_4 catalyst than other solid base catalysts such as CaO, KOH. Mg–Al hydrotalcite.[35] Na_3PO_4 (ref. 28) could achieve beyond 90% yield for the FAMEs biodiesel, so it is feasible and profitable using Na_3PO_4 as s catalysts in novel biodiesel production.

Properties of EGMEML

The properties of obtained EGMEML and standards of diesel and biodiesel were listed in Table 4. In brief, the properties of obtained EGMEML present many similarities with those of diesel and biodiesel, therefore the obtained EGMEML could be deemed as an alternative to diesel.

Conclusions

The effective solid base catalysts were obtained through the simple calcination toward sodium phosphate hydrated, and NaP-400 achieves 90% EGMEML yield in the transesterification reaction to synthesize the novel biodiesel under the optimum conditions: 3.0 EGME/ML molar ratio, 5 wt% catalyst dosage, and 4 h reaction time at 120 °C. Catalytic performance is correlated with the basicity of NaP-T. Meanwhiles, NaP-T possess the good stability and regeneration, the transesterification is governed by chemical step rather than limited by diffusion. And transesterification reaction follows 1st order kinetics. It is inferenced that NaP-T solid base catalysts exhibit the promising prospect in field of novel biodiesel production.

Conflicts of interest

There are no conflicts to declare.

Acknowledgements

References

1 A. Kumar, P. Daw and D. Milstein, *Chem. Rev.*, 2021, **122**, 385–441.

2 P. Intasian, K. Prakinee, A. Phintha, D. Trisrivirat, N. Weeranoppanant, T. Wongnate and P. Chaiyen, *Chem. Rev.*, 2021, **121**, 10367–10451.

3 P. Sudarsanam, E. Peeters, E. V. Makshina, V. I. Parvulescu and B. F. Sels, *Chem. Soc. Rev.*, 2019, **48**, 2366–2421.

4 L. Yang, M. Takase, M. Zhang, T. Zhao and X. Wu., *Renewable Sustainable Energy Rev.*, 2014, **38**, 461–477.

5 M. C. Franssen, P. Steunenberg, E. L. Scott, H. Zuilhof and J. P. Sanders, *Chem. Soc. Rev.*, 2013, **42**, 6491–6533.

6 B. Changmai, C. Vanlalveni, A. P. Ingle, R. Bhagat and S. L. Rokhum, *RSC Adv.*, 2020, **10**, 41625–41679.

7 H. Guo, S. Liu, R. Wang, J. Su, J. Ma and Y. Feng, *Environ. Prog. Sustainable Energy*, 2016, **35**, 241–249.

8 X. Fan, X. Wang, F. Chen, D. P. Geller and P. J. Wan, *Open Fuels Energy Sci. J.*, 2008, **1**, 40–45.

9 S. Liu, W. Chen, Z. Zhu, S. Jiang, T. Ren and H. Guo, *Appl. Sci.*, 2018, **8**, 2303.

10 F. Fan, L. Jia, X. Guo, X. Lu and J. Chen, *Energy Fuels*, 2013, **27**, 5215–5221.

11 G. Gao, Y. Feng, H. Guo and S. Liu, *Energy Fuels*, 2011, **25**, 4686–4692.

12 Y. Li, H. Guo, Z. Zhu, Y. Feng and S. Liu, *Int. J. Green Energy*, 2012, **9**, 376–387.

13 L. Gu, W. Huang, S. Tang, S. Tian and X. Zhang, *Chem. Eng. J.*, 2015, **259**, 647–652.

14 I. M. Atadashi, M. K. Aroua and A. Abdul Aziz, *Renewable Energy*, 2011, **36**, 437–443.

15 S. T. Keera, S. M. El Sabagh and A. R. Taman, *Fuel*, 2011, **90**, 42–47.

16 P. Sudarsanam, R. Zhong, S. Van den Bosch, S. M. Coman, V. I. Parvulescu and B. F. Sels, *Chem. Soc. Rev.*, 2018, **47**, 8349–8402.

17 A. F. Lee, J. A. Bennett, J. C. Manayil and K. Wilson, *Chem. Soc. Rev.*, 2014, **43**, 7887–7916.

18 H. Zhang, L. Chen, Y. Li, Y. Hu, H. Li, C. C. Xu and S. Yang, *Green Chem.*, 2022, **24**, 7763–7786.

19 L. Bournay, D. Casanave, B. Delfort, G. Hillion and J. A. Chodorge, *Catal. Today*, 2005, **106**, 190–192.

20 M. Kouzu, T. Kasuno, M. Tajika, Y. Sugimoto, S. Yamanaka and J. Hidaka, *Fuel*, 2008, **87**, 2798–2806.

21 Y. H. Taufiq-Yap, H. V. Lee, R. Yunus and J. Juan, *Chem. Eng. J.*, 2011, **178**, 342–347.

22 D. A. Molaei and M. Ghasemi, *Fuel Process. Technol.*, 2012, **97**, 45–51.

23 G. Arzamendi, E. Arguiñarena, I. Campo, S. Zabala and L. M. Gandía, *Catal. Today*, 2012, **195**, 54–58.

24 X. Yang, Y. Wang, Y. Yang, E. Feng, J. Luo, F. Zhang, W. Yang and G. Bao, *Energy Convers. Manage.*, 2018, **164**, 112–121.

25 G. Arzamendi, E. Arguiñarena, I. Campo, S. Zabala and L. M. Gandía, *Catal. Today*, 2008, **133**, 305–313.

26 K. V. Yatish, H. S. Lalithamba and R. Suresh, *Sustainable Energy Fuels*, 2018, **2**, 1299–1304.

27 M. Saisriyoot, W. Suksuchot, A. Thanapimmetha, D. Rattanaphra and P. Srinophakun, *Biofuels, Bioprod. Biorefin.*, 2023, **17**, 1174–1182.

28 K. Thinnakorn and J. Tscheikuna, *Appl. Catal., A*, 2014, **476**, 26–33.

29 N. Kaur and A. Ali, *Fuel Process. Technol.*, 2014, **119**, 173–184.

30 W. Xie, H. Peng and L. Chen, *Appl. Catal., A*, 2006, **300**, 67–74.

31 N. Kaur and A. Ali, *Appl. Catal., A*, 2015, **489**, 193–202.

32 F. J. Li, H. Q. Li, L. G. Wang and Y. Cao, *Fuel Process. Technol.*, 2015, **131**, 421–429.

33 O. Özener, L. Yüksek, A. T. Ergenç and M. Özkan, *Fuel*, 2014, **115**, 875–883.

34 M. Mofijur, H. H. Masjuki, M. A. Kalam, A. E. Atabani, M. Shahabuddin, S. M Palash and M. A. Hazrat, *Renewable Sustainable Energy Rev.*, 2014, **28**, 441–455.

35 A. Navajas, I. Campo, A. Moral, J. Echave, O. Sanz, M. Montes, J. A. Odriozola, G. Arzamendi and L. M. Gandía, *Fuel*, 2018, **211**, 173–181.